axis, and the axes **b** and **c** are orthogonal to the axis **a** and make a 22·5 or 15° angle with each other, depending on the class of the rod symmetry (8- or 12-fold, respectively).

3.2. *Two-coloured rod groups*

The two-coloured rod groups containing an 8- or 12-fold axis are presented in Tables 3 and 4, respectively. The first column in these tables gives the symbols of the one-coloured rod groups derived above. The second column gives the symbols of the grey (neutral) groups obtained by additing the anti-identity operation $1'$ to the generators of the one-coloured groups (Belov & Tarkhova, 1956). All the grey groups can accordingly be considered as extensions of the classical groups by means of the group $1'$. Thus, if we denote by C and D the classical and two-coloured rod groups we have that $D = C \otimes 1'$ for the grey groups.

The third column of the tables gives the symbols of the black–white groups D isomorphic with the one-coloured groups C listed in the first columns of the tables. These D groups, which do not contain any antitranslation, may be regarded as extensions of the classical subgroups $C^* \subset C$ of index 2 by means of the antisymmetry point groups G' or antisymmetry groups by modulus $G^{T'}$, *i.e.* as direct, semidirect and quasi-direct products (see *e.g.* Shubnikov & Koptsik, 1974):

$$D = C^* \otimes G', \qquad D = C^* \circledS G' \quad \text{or} \quad D = C^* \odot G^{T'}.$$

Thus, for example, $\not{p}8' = \not{p}4 \otimes 2'$, $\not{p}\underline{12}m'm' = \not{p}\underline{12} \circledS m'$ and $\not{p}8'/m = \not{p}4/m \odot 8' (\mathrm{mod}\ 2)$.

Finally, the two-coloured rod groups in the last column of Tables 3 and 4 contain antitranslations τ'. These groups are obtained from the one-coloured rod groups by additing to the generators of the translation subgroup $T \subset C$ an antitranslation generator τ'. Groups of this type may thus be considered as extensions of the classical groups $C^* = TG$ by means of the group by modulus $\tau' (\mathrm{mod}\ 2\tau) = \{1, \tau'\}$.

References

BELOV, N. V. & TARKHOVA, T. N. (1956). *Kristallografiya*, **1**, 4–13, 619–620 (in Russian). Engl. trans.: *Sov. Phys.–Crystallogr.* (1956), **1**, 5–11, 487–488. Also partial translation of the first paper in *Colored Symmetry* (1964). By A. V. SHUBNIKOV & N. V. BELOV, pp. 211–219. New York: Pergamon Press.

BOYLE, L. L. (1969). *Acta Cryst.* A**25**, 455–459.

BUERGER, M. J. (1963). *Elementary Crystallography.* New York: Wiley.

POND, R. C. & BOLLMANN, W. (1979). *Philos. Trans. R. Soc. London*, **292**, 449–472.

SHUBNIKOV, A. V. & KOPTSIK, V. A. (1974). *Symmetry in Science and Art.* New York: Plenum.

TAVGER, B. A. & ZAITSEV, V. M. (1956). *Zh. Eksp. Teor. Fiz.* **30**, 564–568 (in Russian). Engl. trans.: *Sov. Phys.–JETP* (1956), **3**, 430–436.

VLACHAVAS, D. S. (1980). *Symmetry and Structure of Bicrystals.* PhD Thesis, Univ. of Liverpool.

VLACHAVAS, D. S. (1984). *Acta Cryst.* A**40**, 213–221.

Acta Cryst. (1984). A**40**, 225–228

Experimental Study of X-ray Diffraction under Specular Reflection Conditions

BY A. L. GOLOVIN, R. M. IMAMOV AND S. A. STEPANOV

Institute of Crystallography of the Academy of Sciences of USSR, Leninsky prospect 59, *Moscow* 117333, *USSR*

(*Received* 21 *February* 1983; *accepted* 18 *October* 1983)

Abstract

Results of the experimental study of X-ray diffraction under specular reflection conditions are presented. The experimental arrangement which permits the measurement of the intensity of a specularly reflected diffracted wave with respect to its exit angle to the crystal surface is described. Experimental confirmation of the theory [Afanas'ev & Melkonyan (1983). *Acta Cryst.* A**39**, 207–210] has been obtained for silicon crystals. The angular distributions of the specularly reflected and diffuse intensities have also been studied. The experiments showed the diffuse scattering to be primarily scattering at the back edge of the sample.

The diffraction under specular reflection conditions occurs when an X-ray beam is directed into a crystal at a small glancing angle, φ, of incidence comparable with the critical angle of specular reflection and, simultaneously, if the conditions of Laue case diffraction for the planes normal to the surface are met.

As was shown earlier (Marra, Eisenberger & Cho, 1979; Afanas'ev & Melkonyan, 1983), two specularly

0108-7673/84/030225-04$01.50

reflected waves leave the crystal through the entrance surface in this case. The former wave satisfies the specular reflection condition, making an angle φ with the surface. The latter one being the specular component of the diffracted wave, makes an angle $2\theta_B$ with the specularly reflected wave. The value of the exit angle φ_h made by this wave with the surface depends on how exactly the Bragg condition is met. In particular, the following relation occurs:

$$\alpha = \varphi^2 - \varphi_h^2, \tag{1}$$

$$\alpha = -2 \sin (2\theta_B)\delta\theta, \tag{2}$$

the parameter determining the deviation from the Bragg condition.

Analytical expressions defining the specularly reflected diffracted intensity dependence on φ and α have been obtained by Afanas'ev & Melkonyan (1983). It has also been shown that at certain values of the glancing angle φ the reflection-coefficient maximum is close to unity.

The difficulty of experimental realization of diffraction under specular reflection conditions is connected with the necessity of X-ray beam collimation in two mutually perpendicular planes: through the glancing angle φ (of the order of minutes of arc) and through the angular deviation $\delta\theta$ from the exact Bragg angle (of the order of seconds of arc).

The use of (1) enables one to avoid the problem and to give up the collimation through the angle $\delta\theta$ (*i.e.* on α). Then, instead of a single specularly reflected wave some set of the waves will exit resulting in an intensity distribution depending on the angle φ_h. Recording this distribution as a function of the angle φ_h, *i.e.* introducing collimation through the exit angle φ_h, for example, with an accuracy of 30″, one has an accuracy in $\delta\theta$ of

$$\delta\theta = \frac{\varphi\delta\varphi_h}{\sin (2\theta_B)}.$$

To solve this problem experimentally a new experimental scheme was proposed by Golovin & Imamov (1983). This scheme allows one to measure the dependence of specularly reflected intensity on φ in the integral mode, *i.e.* with integral registration through all exit angles φ_h, which is the simplest to perform.

The results of such measurements with silicon single crystals were presented (Golovin & Imamov, 1983). Integral curves can be used for obtaining preliminary information on the surface layers. However, to obtain detailed information on these layers measurements in differential mode with a narrow interval at the exit angles are required. The angular dependences of intensity measurements in the differential mode for a perfect silicon single crystal are presented below.

A sketch of the experimental set-up is shown in Fig. 1. An X-ray beam from a 1.2 kW X-ray source was directed at a monochromator crystal at the Bragg angle [silicon (220)–symmetrical reflection in the Bragg case for Cu $K\alpha$ radiation was used). The beam reflected by the monochromator crystal was incident on the sample at a small glancing angle φ and diffracted on the (220) planes normal to the entrance surface.

There was a slit (see Fig. 1, no. 3) between the monochromator crystal and the sample to distinguish a $K\alpha_1$ line from the total X-ray spectrum. The slit size defined the width of the incident-beam front (20–100 μm). The beam divergence in the horizontal plane, in our experiment about 6″, was defined by the angular half-width of the monochromator rocking curve. In the vertical plane collimation was not provided and the divergence of the X-ray beam was limited by the design of the spectrometer. In the experimental set-up the vertical divergence was about 1°.

The angular dependences were measured by a goniometer based on a triple-crystal spectrometer (TRS).

Counters 1 and 2 were set on bars rotating about the goniometer axis.

The first counter was supplied with a slit for registering diffracted waves with different exit angles φ_h from the crystal surface. The slit had an alterable window which was used to distinguish a rather narrow interval from the whole band of φ_h angles. Since the axis around which the angle was to be measured made an angle $2\theta_B$ with the goniometer axis, the turn of counter 1 around the goniometer axis by an angle

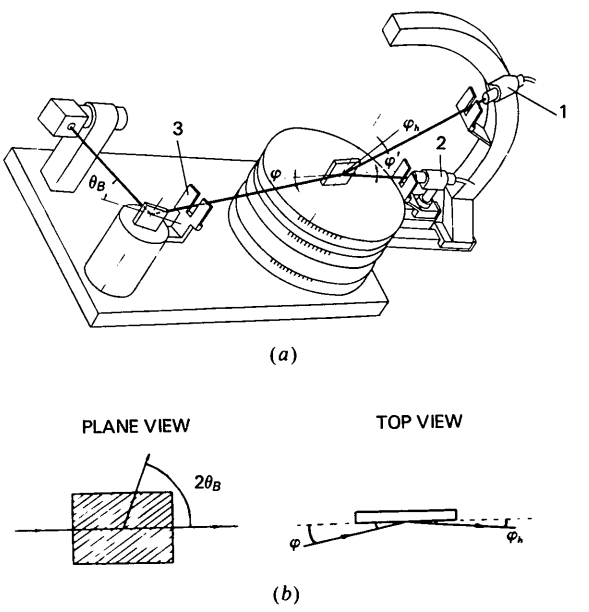

Fig. 1. X-ray optics scheme of the experimental set-up. General view of the experimental arrangement: 1 counter for registration of specularly reflected diffracted intensity; 2 counter for registration of specularly reflected and forward-beam intensities; 3 slit. (*b*) Scheme of beam trajectory.

$\delta\varphi_1$ corresponded to a change of φ_h of

$$\delta\varphi_h = \delta\varphi_1 \cos 2\theta_B.$$

In the experiment only part of the beam was incident onto the sample, the remaining (forward) beam passing it by and forming a reference signal for counter 2. Counter 2 with a removable slit 50 μm in width was used for investigation of the X-ray intensity angular spread in the direction of the forward beam and specularly reflected beam. The angular position φ' of detector 2 was measured around the goniometer axis from the forward-beam direction, and the direction of the specular reflected beam in this reference frame corresponded to $\varphi' = 2\varphi$.

A multichannel analyzer NTA-1024 working in a multichannel mode was attached to the system as a recording device. The duration of pulses accumulation in each channel was 2 s.

The experiments were carried out with a perfect silicon single crystal with (100) surface orientation after standard mechanical and chemical surface treatments. The deviation of surface orientation from (100) was less than ±15′. Crystal diameter was 20 mm, thickness 1 mm.

Typical diffractograms measured with detector 1 and showing dependences of specular reflected diffracted intensity on φ_h for different glancing angles of incidence φ (4, 12 and 26′) are presented in Fig. 2. The resolution at φ_h was not worse than 3′ because the slit size at counter 1 was 50 μm. Fig. 2 shows the calculated curves which were obtained on the basis of the theory (Afanas'ev & Melkonyan, 1983), averaging through the angle φ_h over 3′ and with an allowance for a relative contribution of polarizations $I_\sigma/I_\pi = \cos 2\theta_B = 0.7$.

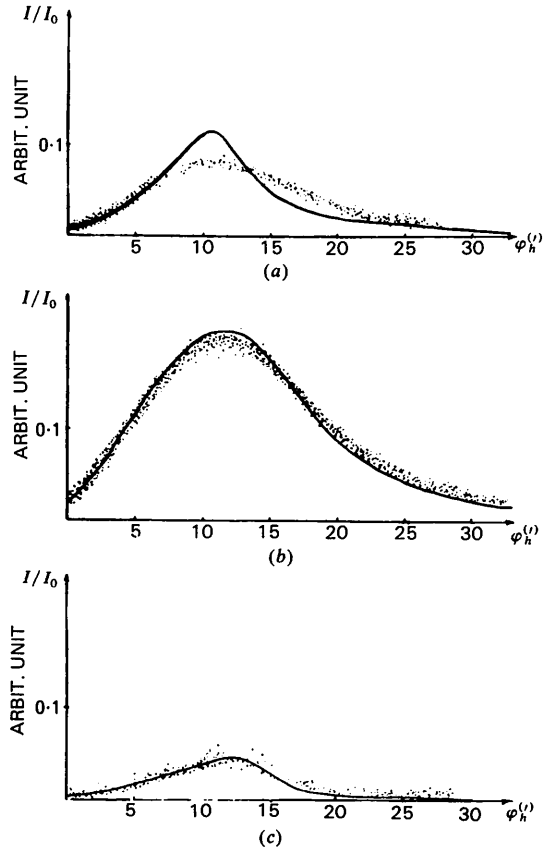

Fig. 2. Typical diffractograms for silicon samples and different angles φ of incidence. (*a*) $\varphi = 4'$, (*b*) $\varphi = 12'$, (*c*) $\varphi = 26'$.

$$I(\varphi, \varphi_h) \simeq \sum_{j=\delta,\pi} c_j \int_{\varphi_h - 0.5\Delta\varphi_h}^{\varphi_h + 0.5\Delta\varphi_h} P^s_{hj}(\varphi, \varphi_h)(2\varphi_h)\, \mathrm{d}\varphi_h,$$

where $c_\pi = 1/(1+\cos 2\theta_B)$, $c_\delta = c_\pi \cos 2\theta_B$, $\Delta\varphi_h = 3'$, $(2\varphi_h)$ being the factor due to (1). The value $P^s_{hj}(\varphi, \varphi_h)$ is the reflection coefficient calculated by Afanas'ev & Melkonyan (1983). Theoretical and experimental curves show satisfactory agreement in shape, relationship of intensities and the intensity maxima angular position.

However, some differences are evident. First of all, there is disagreement in theoretical and experimental half-width values. It can be especially well seen in the spectrum corresponding to the glancing angle $\varphi = 4'$; at this glancing angle the X-ray penetration depth is small, less than 100 Å, and there are many imperfections in subsurface layers of real crystals. Besides, a possible disorientation of the surface from (100) and the influence of surface unevenness were not taken into account.

The angular distributions of the forward-beam intensity both for the case when the sample is mounted on the goniometer and makes different angles with the beam and for the case without the sample are presented in Fig. 3. Distributions of specularly reflected intensity are also presented. One can see

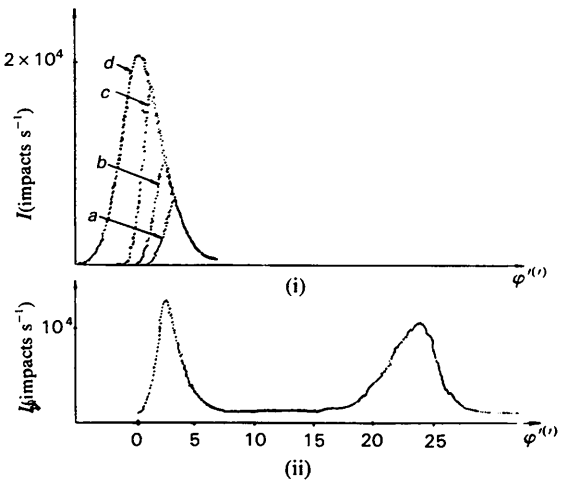

Fig. 3. (i) Distribution of the forward-beam intensity with the crystal making different angles with the beam: (*a*) $\varphi = 26'$, (*b*) $\varphi = 12'$, (*c*) $\varphi = 0'$, (*d*) without the crystal. (ii) Distributions of specularly reflected and diffuse intensities for $\varphi = 12'$.

that the specular intensity maximum corresponds to the angle φ' equal to 2φ. Besides the specularly reflected intensity diffuse scattering is observed, which might be caused by the surface unevenness and by the back edge of the sample. It is registered most clearly at the angle $\varphi > 14'$, *i.e.* in the case when the specularly reflected intensity may be neglected (see Fig. 4*a*). The experiments showed a weakening of the diffuse intensity when only part of the incident beam reached the crystal back edge (see Fig. 4*b*). This fact showed that the main contribution to the diffuse scattering was due to the scattering at the sample back edge.

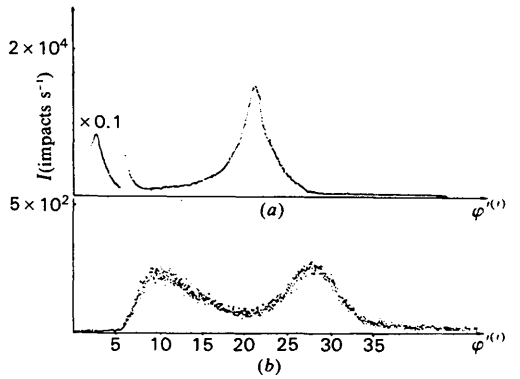

Fig. 4. Distribution of the diffuse intensity for $\varphi = 16'$. (*a*) The crystal covers half of the beam (the forward wave can be seen); (*b*) the crystal covers the whole beam (no forward beam).

Thus, the intensity measurement of the specularly reflected diffracted wave with its exit-angle change has been experimentally realized and the main statements of the theory (Afanas'ev & Melkonyan, 1983) have been confirmed.

The authors express their sincere thanks to Professor A. M. Afanas'ev for his unfailing attention to the work and fruitful discussions, and to D. Novikov for the help in conducting the experiments.

References

AFANAS'EV, A. M. & MELKONYAN, M. K. (1983). *Acta Cryst.* A**39**, 207–210.

GOLOVIN, A. L. & IMAMOV, R. M. (1983). *Phys. Status Solidi A*, **77**, K91–K94.

MARRA, W. C., EISENBERGER, P. & CHO, A. Y. (1979). *J. Appl. Phys.* **50**, 6927–6933.

Acta Cryst. (1984). A**40**, 228–240

Diffuse Scattering in Disordered Ternary Alloys: Neutron Measurements of Local Order in a Stainless Steel $Fe_{0.56}Cr_{0.21}Ni_{0.23}$

BY P. CENEDESE

Institut Laue–Langevin, 156*X*, 38042 *Grenoble CEDEX, France*

AND F. BLEY* AND S. LEFEBVRE

CECM, 15 *rue G. Urbain*, 94400 *Vitry/Seine, France*

(*Received* 24 *May* 1983; *accepted* 1 *November* 1983)

Abstract

The local atomic arrangement in the stainless-steel alloy $Fe_{0.56}Cr_{0.21}Ni_{0.23}$ has been investigated by thermal neutron diffuse scattering from single crystals. The variation of contrast has been obtained by isotopic substitution: three single crystals of different isotopic compositions have been used. The Warren–Cowley parameters of the three heterogeneous pairs have been determined. It is shown that ordering occurs between Ni and Cr atoms. The correlation lengths are small and are of about one cell length. The static displacements are shown to be small. Analysis procedures of diffuse scattering from ternary alloys are developed from neutron scattering and in the Appendix for X-ray scattering.

I. Introduction

During the last ten years, considerable developments have been made in analysing diffusely scattered intensity from mono-crystalline binary alloys since this provides the volume averaged pair atomic correlations by Fourier transformation. These can then be used to model important physical properties such as thermodynamic (pair interaction potentials) and mechanical properties and electrical resistivity.

On the other hand, no direct determination of short-range ordering has been made on multicomponent solid solutions. As a consequence, evolutions of solid

* Present address: INPG–LTPCM (LA29)–ENSEEG, Domaine Universitaire, BP 75, 38042 St Martin d'Hères, France.

0108-7673/84/030228-13$01.50